

REPORT



## Rabbits transgenic for human IgG genes recapitulating rabbit B-cell biology to generate human antibodies of high specificity and affinity

Francesca Ros<sup>a</sup>, Sonja Offner<sup>a</sup>, Stefan Klostermann<sup>b</sup>, Irmgard Thorey<sup>a</sup>, Helmut Niersbach<sup>c</sup>, Sebastian Breuer<sup>a</sup>, Grit Zarnt<sup>a</sup>, Stefan Lorenz<sup>a</sup>, Juergen Puels<sup>d</sup>, Basile Siewe<sup>e</sup>, Nicole Schueler<sup>a</sup>, Tajana Dragicevic<sup>a</sup>, Dominique Ostler<sup>a</sup>, Imke Hansen-Wester<sup>f</sup>, Valeria Lifke<sup>g</sup>, Brigitte Kaluza<sup>a</sup>, Klaus Kaluza<sup>a</sup>, Wim van Schooten<sup>h</sup>, Roland Buelow<sup>h</sup>, Alain C Tissot<sup>a\*</sup>, and Josef Platzer<sup>a\*</sup>

<sup>a</sup>Roche Pharmaceutical Research and Early Development, Large Molecule Research, Roche Innovation Center Munich, Penzberg, Germany; <sup>b</sup>Roche Pharmaceutical Research and Early Development, Informatics, Roche Innovation Center Munich, Penzberg, Germany; <sup>c</sup>Roche Pharmaceutical Research and Early Development, Pharmaceutical Sciences, Roche Innovation Center Munich, Penzberg, Germany; <sup>d</sup>TÜV SÜD Product Service GmbH, Munich, Germany; <sup>e</sup>THE JACKSON LABORATORY JMCRS, Sacramento, CA, USA; <sup>f</sup>Supplier Quality Management, Global External Quality Roche Diagnostics GmbH, Penzberg, Germany; <sup>g</sup>Personalized Healthcare Solution, Immunoassay Development and System Integration, Roche Diagnostics GmbH, Penzberg, Germany; <sup>h</sup>Teneobio, Inc., Newark, CA, USA

### ABSTRACT

Transgenic animals incorporating human antibody genes are extremely attractive for drug development because they obviate subsequent antibody humanization procedures required for therapeutic translation. Transgenic platforms have previously been established using mice, but also more recently rats, chickens, and cows and are now in abundant use for drug development. However, rabbit-based antibody generation, with a strong track record for specificity and affinity, is able to include gene conversion mediated sequence diversification, thereby enhancing binder maturation and improving the variance/selection of output antibodies in a different way than in rodents. Since it additionally frequently permits good binder generation against antigens that are only weakly immunogenic in other organisms, it is a highly interesting species for therapeutic antibody generation. We report here on the generation, utilization, and analysis of the first transgenic rabbit strain for human antibody production. Through the knockout of endogenous IgM genes and the introduction of human immunoglobulin sequences, this rabbit strain has been engineered to generate a highly diverse human IgG antibody repertoire. We further incorporated human CD79a/b and Bcl2 (B-cell lymphoma 2) genes, which enhance B-cell receptor expression and B-cell survival. Following immunization against the angiogenic factor BMP9 (Bone Morphogenetic Proteins 9), we were able to isolate a set of exquisitely affine and specific neutralizing antibodies from these rabbits. Sequence analysis of these binders revealed that both somatic hypermutation and gene conversion are fully operational in this strain, without compromising the very high degree of humanness. This powerful new transgenic strategy will allow further expansion of the use of endogenous immune mechanisms in drug development.

### ARTICLE HISTORY

Received 18 February 2020  
Revised 1 October 2020  
Accepted 23 October 2020

### KEYWORDS

Rabbit; human immunoglobulins; IgG; transgenic; immune repertoire; gene conversion; somatic hypermutation; diversity; functionality; affinity; specificity; humanness; drug discovery

### Introduction

Monoclonal antibodies are an important and expanding therapeutic modality that has profoundly affected drug development in therapeutic areas such as oncology and immunology. Approved (and marketed) antibody drugs consist mainly of IgG class humanized or human antibodies. Investigational antibody therapeutics in clinical trials are typically human antibodies,<sup>1</sup> with a humanness of 90–100%,<sup>2</sup> and are derived from *in vitro* antibody libraries using display technologies or *in vivo* from immunized transgenic mice.

Engineered animals using human antibody sequences for generation of their endogenous humoral immune response have allowed pharmaceutical research to harness the tremendous power of the adaptive immune system. *In vivo* sequence diversification, antigen-driven somatic hypermutation, and

numerous quality control checkpoints, such as positive and negative selection mechanisms, ensure the nonrandom selection and enrichment of B cells that produce antibodies with therapeutically desirable properties.<sup>2</sup> Ideal antibody candidates are often required to bind with high affinity to a specific epitope, cross-react to a non-human orthologue, lack binding to human paralogues, and fulfill stringent drug development criteria; developable therapeutic antibodies are rare events in the immune repertoire.

Rabbit monoclonal antibodies are used extensively for diagnostic applications due to the high affinity and specificity that can be achieved,<sup>3</sup> specially toward antigens that are weakly immunogenic in mice. They are also highly preferred for therapeutic drug development since antibodies that are cross-reactive with the respective murine orthologs are more frequently produced in rabbits than in mice due to

**CONTACT** Francesca Ros  [francesca.ros@roche.com](mailto:francesca.ros@roche.com)  Roche Pharmaceutical Research and Early Development, Large Molecule Research, Roche Innovation Center Munich, Penzberg, Germany; Alain C Tissot [alain.tissot@roche.com](mailto:alain.tissot@roche.com); Josef Platzer [josef.platzer@roche.com](mailto:josef.platzer@roche.com).

\*These authors are contributed equally to this work

 Supplemental data for this article can be accessed on the [publisher's website](#).

© 2020 Taylor & Francis Group, LLC

This is an Open Access article distributed under the terms of the Creative Commons Attribution-NonCommercial License (<http://creativecommons.org/licenses/by-nc/4.0/>), which permits unrestricted non-commercial use, distribution, and reproduction in any medium, provided the original work is properly cited.

immunological tolerance.<sup>4</sup> One reason for these outstanding features may lie in the B-cell ontogeny, which is different in rabbits compared to humans, mouse, and rat. The neonatal B-cell repertoire in rabbits is generated by lymphopoiesis in fetal liver and bone marrow and is limited by preferential Heavy-Chain Variable Regions (VH1) gene segment usage. Between 4 and 8 weeks after birth, a complex primary antibody repertoire is developed by somatically diversifying the neonatal repertoire through somatic hypermutation and a somatic gene conversion (GC)-like mechanism in gut-associated lymphoid tissue (GALT).<sup>5–7</sup> The primary antibody repertoire is subsequently modified during antigen-dependent immune responses in which VDJ genes further diversify both by somatic hypermutation and GC (the secondary repertoire) ensuring a tight fit to the antigen of interest.

Recently, the comprehensive rabbit antibody repertoire was analyzed with next-generation sequencing technology. The somatic mutations in rabbit VH and VK (Variable region Kappa Chain) regions are higher than in their human and mouse counterparts. Rabbit VH regions accumulate over 60% more mutations than the respective human or mice VH regions. Also, the rabbit VK regions show this feature especially in framework regions (FR)-1 and FR-3. A higher degree of somatic mutations of the repertoire of rabbit VK regions compared with humans and mice could also compensate for the limited diversity of the germline genes used to generate the rabbit functional repertoire.<sup>8</sup>

Genomically, rabbits are very well characterized. The rabbit immunoglobulin heavy chain (IgH) locus contains over 200 IgH variable germline genes. Of them, over 50% are found to be “non-functional.” In addition, more than 50 Ig (immunoglobulin) Kappa V and 17 Ig Lambda V functional genes were identified with genomic sequencing (ImMunoGeneTics information system® (IMGT) database; <http://www.imgt.org>). The diversity of rabbit VH repertoire is more limited compared to other species, but the V light (VK) repertoire is more diverse than that in mice and humans.<sup>9,10</sup>

We describe here for the first time the generation of transgenic rabbits producing human antibodies with VDJ gene rearrangements that are capable of further somatic hypermutation and GC being necessary for efficient antibody maturation. Several known key genes for the regulation of a very diverse and matured B-cell and antibody repertoire were included in a species-specific way to overcome challenges like

outnumbering of the transgenic B-cell count or hampering the maturation of the transgenic B-cell repertoire. The combination of the knockout of the crucial rabbit IgM and the introduction of additional transgenes like human Bcl2, as well as CD79a and CD79b, were applied to enable the full B-cell cycle maturation in the transgenic rabbit.

The performance of the transgenic rabbits was evaluated using a target for angiogenesis in oncology, bone morphogenetic protein 9 (BMP9), as the antigen for immunization.<sup>11,12</sup> Immunization and lead identification were tailor-made to obtain lead candidates with desired specifications. These were cross-reactive to cynomolgus and murine BMP9, with high-affinity binding to human BMP9 in the subnanomolar range and no binding to the related BMP10, as well as subnanomolar blocking of the BMP9-Alk1 interaction. A very diverse set of human antibodies with the desired properties could be successfully retrieved from the rabbits transgenic for human immunoglobulins.

## Results

### Generation of transgenic rabbits expressing human IgG antibodies

For the generation of transgenic rabbits, superovulated females were mated with males carrying the Basilea mutation, a strain naturally deficient in the rabbit kappa light chain.<sup>13</sup> Linearized DNA coding for the fully human heavy chain (FHH1.1-bcl2), for the fully human light chain construct (FHLC1.1), or an equimolar mixture of human CD79a/b bacterial artificial chromosome (BAC) DNA were microinjected into oocytes. The final configurations of the FHH1.1-bcl2 and FHLC1.1 constructs are illustrated in [Figure 1](#).

For the heavy chain, eight functional human gene segments of the VH3 family, separated by rabbit introns and spacers and preceded by rabbit promoters and leader peptides, were inserted upstream of a rabbit D locus flanked by a fully human Junction segment Heavy Chain (JH) locus. The rabbit constant regions of IgG and IgM were replaced by the human counterparts, respectively: the human IgG1 and human IgM constant regions, followed downstream by rabbit C $\epsilon$ , C $\alpha$ 4 constant and hs1,2 and 4 enhancer regions. A F2A (self-cleaving peptide) – human Bcl2 gene (codon optimized) cassette, was fused to the rabbit membrane exon M2 of the human C $\mu$  locus. A 235 Kb Asi SI–Asc I fragment was isolated for microinjection. The D locus was not humanized mainly for two

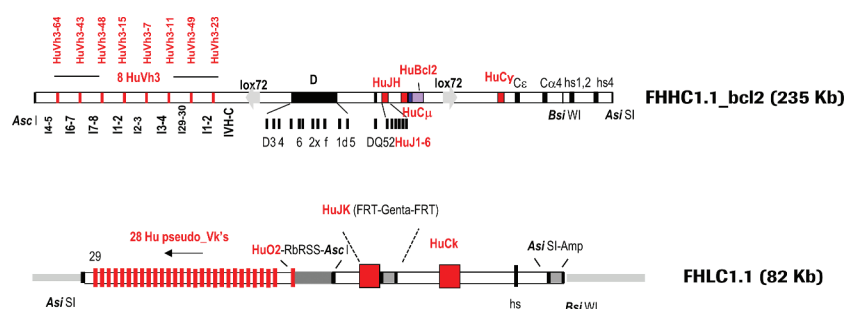


**Figure 1.** Final configuration of human heavy (FHH1.1-bcl2) and light (FHLC1.1) chain constructs used for the generation of transgenic rabbits expressing human IgG antibodies. Marked in red are human segments included in the constructs.

reasons: 1) Practically, it was impossible to integrate the large size of the entire human DH locus into the transgenes, and 2) Strategically, we wanted to take advantage of the high diversity of the rabbit D elements.

For the light chain, 29 human kappa V genes (28 pseudogenes and 1 fully functional gene segment VK-O2 flanked downstream by a rabbit RSS region from the V kappa 2 chain) separated by chicken Ig Kappa 1 spacers were located upstream of a fully human Junction segment Kappa Chain (JK) locus. The rabbit constant region of the kappa chain was replaced by the human IgK1 counterpart. Rabbit enhancer regulatory elements were included in the microinjected construct. An 80 Kb Asi SI fragment was isolated for microinjection. As mentioned in the Materials and Methods section, rationale and details on design of FHHCl.1-bcl2 and FHLC1.1 constructs are described in Patent Number US RE47, 131 E and on Supplementary material (Part 1, Fig. 14–18; numbering of figures and tables in the supplementary materials starts with Fig. 14 and Table 5, respectively).

Transgenic founders and their first-generation offspring were analyzed by: 1) PCR for the presence of both variable and constant human IgG regions, 2) fluorescent *in-situ* hybridization for single integration sites of the human heavy and light chain transgenes on chromosomes other than those harboring the respective endogenous loci, and 3) quantitative PCR for single copy integration of human heavy and light chain transgenes (Supplementary material, Table 5, Part 3). The selected transgenic founders listed in the table gave rise to offspring which, after being bred with each other and with animals carrying rabbit IgM knockout mutations,<sup>14</sup> were able to produce a diversified pre-immune repertoire of human antibody sequences (data not shown). The three transgenic rabbits selected for BMP9 immunization were derived from breeding combining all necessary genotypes: 1) FHHCl.1-bcl2 (hemizygous or homozygous); 2) FHLC1.1 (homozygous); 3) human CD79a/b (homozygous); and 4) rabbit IgM knockout (homozygous or compound heterozygous). Details on genotype specifications are shown in Table 1.

### Characterization of the transgenic B-cell compartment by preimmune FACS analysis

At 15–19 weeks after birth, the peripheral B-cell population of human IgG transgenic rabbits was characterized by fluorescence-activated cell sorting (FACS) analysis (Figure 2, Table 2).

As described in Flisikowska et al.,<sup>14</sup> only ~0.1 to 0.7% of peripheral blood mononuclear cells (PBMCs) stained positive for rabbit IgM, demonstrating that rIgM had indeed been knocked-out. In control wild-type animals, ~50% of PBMCs were positive for rIgM and transgenic rabbits delivered ~8–18% B cells positive for huIgM. Both frequencies of IgM-positive B cells are typical for rabbit blood, implying that the B-cell-knockout trait of the rIgM-negative rabbits could be rescued in the huIgM-positive transgenic animals.

However, there were two populations of B-cells displaying cell surface IgG: 1) the major population of the B cells produced a chimeric antibody consisting of a human VDJ region, a human LC, but a rabbit IgG Fc part as confirmed by the sequence analysis (data not shown), and 2) a very small population of B cells generating a fully human IgG1. The polyclonal anti-rIgG Fc antibody used for the FACS analysis and for the following single B-cell sort detects both the rabbit as well as the human IgG Fc on the B cell surface. The rabbit IgG Fc was detected with a higher intensity than the human IgG1 Fc. The presence of the fully human IgG1 on the cell surface of a few transgenic B cells was proved by a detection antibody that specifically binds to human IgG1 Fc, but not to rabbit IgG Fc.

Other well-defined B cell-specific markers are human CD79a and human CD79b, constituting the transgenic B cell receptor together with huIgM. The introduction of the human CD79a/b genes was essential for cell surface expression of huIgM. Transgenic animals without these genes express huIgM exclusively intracellularly (Supplementary material Fig. 19, Part 7) irrespective of the presence of the human light chain (enzyme-linked immunosorbent assay (ELISA) data not shown). Transgenic B cells expressing huLC kappa constitute 15–18% of all PBMCs. The frequencies of the human B-cell receptor markers human CD79a/b as well as huLC kappa matched the frequencies of the huIgM-positive B cells (9–18% of all PBMCs). Overall, all human transgenes were expressed in a rabbit wild-type like frequency on the transgenic B-cell surface.

### Preimmune ELISA Analysis

The capability of the transgenic B cells to build a functional humoral immune response was confirmed by measuring serum levels of different immune globulins at various ages. As shown in Table 3, the three transgenic rabbits used for immunization had robust human Ig serum levels irrespective of whether they

**Table 1. Genotype specifications of immunized transgenic animals.** Immunized rabbits (Ali/Bas background) were homozygous (+/+) for hulgK (FHLC1.1) and huCD79a/b (CD79ab) and hemizygous (±) for hulgG (FHHCl.1-bcl2) transgenes. Founders 1007658 and 1007340 differ on the chromosomal insertions of the FHHCl.1-bcl2 transgene. For the rIgM KO (KOΔ: deletion mutation, KOI: insertion mutation), animals were either homo- or compound heterozygous. For details on KO nomenclature please refer to Flisikowska et al.<sup>14</sup>

Rabbit ID	Transgenic	Sex	ID Mother	ID Father	Tg Line Spec	Ali	Bas
500350	F5	Female	500294	500280	23223 (FHLC1.1+/+), 1007658 (FHHCl.1-bcl2±), 1016657 (CD79ab+/+), 22826 (IgM-KOΔA1±), 22830 (IgM-KOΔA7±)	+/+	+/+
500370	F4	Female	500180	500261	23223 (FHLC1.1+/+), 1007658 (FHHCl.1-bcl2+/+), 1016657 (CD79ab+/+), 22830 (IgM-KOΔA7-/-)	+/+	+/+
500376	F5	Female	500294	797	23223 (FHLC1.1+/+), 1007340 (FHHCl.1-bcl2±), 1016657 (CD79ab+/+), 22826 (IgM-KOΔA1±), 25039 (IgM-KOIA1±)	+/+	+/+

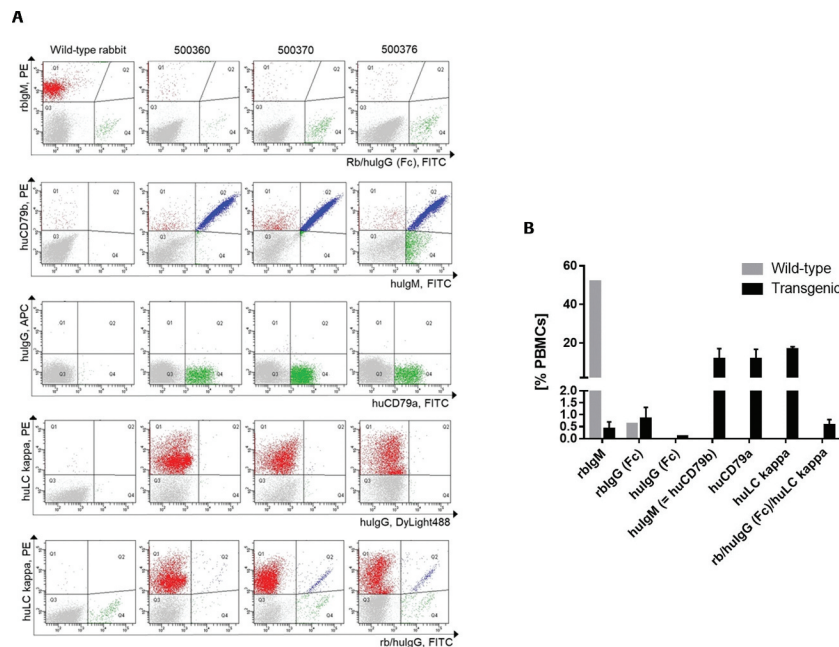


**Figure 2.** (a) Characterization of the peripheral B-cell compartment of wild-type and transgenic rabbits using FACS analyses. FACS dot plots per column show representative profiles of peripheral blood mononuclear cells (PBMCs) of one wild-type rabbit and three transgenic rabbits (500350, 500370, 500376). The FACS dot plots in each row represent five different FACS double staining of live PBMCs using the cell-surface markers indicated. (b) Frequencies of different B-cell populations. The B cell frequency is measured as percentage of the count of gated cell-surface marker X-positive B cells of all PBMCs.

**Table 2.** Frequency of B-cell populations (%) of wild-type and transgenic rabbits.

	Wild-type	Transgenic		
		500350	500370	500376
rblgM	51.9	0.7	0.1	0.4
rblgG (Fc)	0.6	1	1.2	0.3
hulgG (Fc)	0	0.1	0.1	0.1
hulgM (= huCD79b)	0	8.2	17.9	9.3
huCD79a	0	8.6	17.5	8.7
huLC kappa	0	14.8	17.3	17.6
rb/hulgG (Fc)/huLC kappa	0	0.7	0.7	0.3

were hemizygous or homozygous for the human Ig transgenes (confirmed by the respective ELISA results from other transgenic animals, data not shown).

Clearly, no rabbit IgM could be detected in the sera, whereas robust human IgM, IgG and human kappa levels were detected in all animals. In line with the FACS analysis, a significant level of antibodies displaying a rabbit IgG Fc was also detected by ELISA, and interestingly the concentration of this chimeric

antibody increased over time, whereas the amount of antibodies containing a human IgG Fc decreased.

### Immunization

Transgenic rabbits were subjected to three basic immunizations with recombinant human BMP9 pro-domain at weekly intervals and were further boosted at monthly intervals.

As shown in Figure 3, all three transgenic rabbits selected for immunization developed robust and increasing titers of antigen-specific antibodies during the course of the six immunizations. While antigen-specific antibodies containing the human IgG Fc from the transgene were clearly detectable in each animal, the majority of the antigen-specific antibodies contained rabbit IgG Fc domains. The chimeric nature of most of the retrieved antibodies did not represent an obstacle for antibody generation and isolation, as the constant domain of an antibody can easily be exchanged by recombinant technology.

**Table 3.** Prior to immunization with BMP9, serum from the three selected transgenic rabbits was analyzed for the presence of rabbit and human IgG immunoglobulin chains at different ages.

Rabbit ID	Tg Line Spec	Serum conc., µg/ml					age, weeks
		hulgG	hulgM	rblgG	rblgM	hukappa	
500350	23223 (FHLC1.1+/+), 1007658 (FHHC1.1-bcl2±), 1016657 (CD79ab+/+), 22826 (IgM-KOΔA1±), 22830 (IgM-KOΔA7±)	11	bdl	10	bdl	33	8
		73	70	810	bdl	380	16
		bdl	84	840	bdl	220	28
500370	23223 (FHLC1.1+/+), 1007658 (FHHC1.1-bcl2+/+), 1016657 (CD79ab+/+), 22830 (IgM-KOΔA7-/-)	810	23	1400	bdl	3300	8
		270	150	1400	bdl	2200	12
		17	180	3800	bdl	330	15
		6	170	680	bdl	3700	24
500376	23223 (FHLC1.1+/+), 1007340 (FHHC1.1-bcl±), 1016657 (CD79ab+/+), 22826 (IgM-KOΔA1±), 25039 (IgM-KOIA1±)	2900	51	560	bdl	3100	8
		1800	1400	1200	bdl	5700	12
		47	210	4300	bdl	870	15
		62	1100	3200	bdl	11800	24

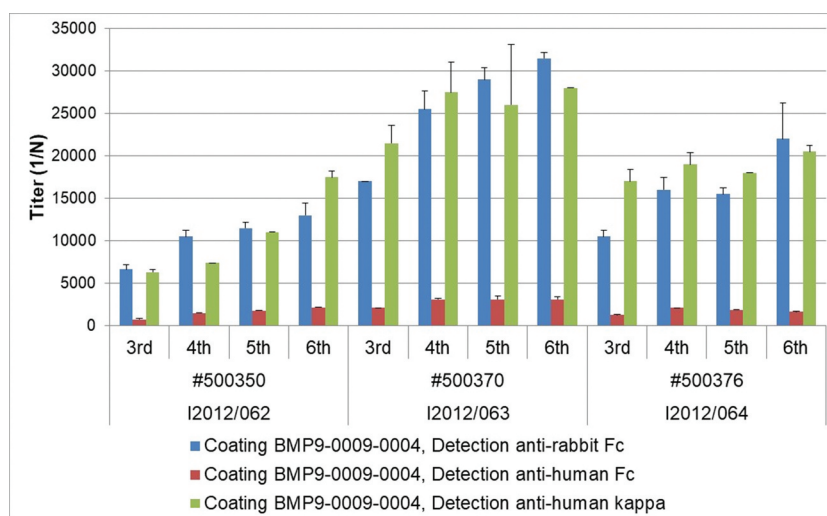


**Figure 3.** ELISA titer for antigen specificity. Serum from the three immunized transgenic rabbits was analyzed for the presence of rabbit and human IgG immunoglobulin chains during the course of immunization.

### Generation of monoclonal rabbit antibodies binding to BMP9

We used pro-BMP9 in adjuvant to raise an immune response and generate a B cell repertoire in wild-type and transgenic rabbits, with the objective to isolate a collection of specific antibodies inhibiting BMP9 binding to its receptor and subsequent signaling. The choice of the antigen was motivated by the possibility to inhibit all forms of BMP9, being aware that after processing pro-BMP9 is present as a complex which dissociates upon receptor binding.<sup>12</sup>

After three immunizations, individual B-cell clones (antibody-secreting cells) were isolated by the B-cell cloning process using peripheral B cells of rabbits immunized against BMP9, as described in Seeber et al.<sup>15</sup> The antibody detecting human IgG (huIgG) was specific for the human Fc, whereas the antibody binding to the rabbit IgG Fc was cross-reactive to huIgG. This enabled the detection of the two transgenic B-cell populations displaying human VK and VH IgGs, namely the one with huIgG Fc and the one with rbIgG Fc, facilitating the B-cell sorting step of the B-cell cloning approach.

In particular, the Rabbit/Human IgG and huLC kappa-double positive B cells were used for single B-cell sorting to be processed in the B-Cell Cloning approach as described in Seeber et al.<sup>15</sup> Common frequencies of this sorted B-cell populations comprised 0.3 to 0.7% of all PBMCs.

In total, 10079 individual IgG-positive B cells from the two blood samples of each of the three BMP9-immunized wild-type rabbits and 9841 individual IgG/huCk-double-positive B cells from the two blood samples of each of the three BMP9-immunized transgenic rabbits were deposited in 96-well plates to induce B-cell proliferation and IgG secretion during B-cell culture. The identification of anti-BMP9 specific antibodies was achieved by high throughput screening using three different ELISA-based binding assays discriminating anti-human, mouse, and cynomolgus BMP9 cross-specific antibodies (Figure 4). All six immunized rabbits delivered BMP9-specific B-cell clones producing sufficient IgG over a broad range of concentrations (0.012 µg/

ml to >60 µg/ml). The average frequency of IgG-producing B-cell clones from the BMP9-immunized transgenic rabbits (40–53%) was comparable to the IgG frequency of the wild-type rabbits (30–50%). Of the 7709 IgG-positive supernatants, 4372 (57%) derived from the transgenic rabbits and 3337 (43%) from the wild type. Also, the percentage of IgG-positive supernatants binding to the human BMP9 protein was quite similar between the transgenic (9–20%) and the wild-type rabbits (10–23%). In summary, the results of the primary screening show that the yield of BMP9-binding antibodies from the wild-type and the transgenic rabbit strain is very similar. Differences of the immune response of individual animals were evident, but were observed both in wild type and in the transgenic strain.

We proceeded to analyze the cross-reactivity to cynomolgus or murine BMP9 with the B-cell supernatants of the transgenic rabbits. On average, 7–17% of the IgG-positive supernatants showed binding to the cynomolgus BMP9 antigen and 6–12% showed binding to the murine BMP9 antigen depending on the individual transgenic animal. Based on the counts for human BMP9 protein binders, 78% and 53% of these antibodies were positive for binding to cynomolgus and murine BMP9 antigen, respectively. Over 44% of the human BMP9-positive antibodies were even triple reactive to human/cynomolgus/murine BMP9, representing the most interesting population of antibodies with regard to their use for further animal studies.

### Secondary screening: IC50 and inhibition properties

A selection of 107 primary hits from the transgenic strains was amplified by B-cell PCR, and transfected in mammalian HEK293 cells for expression and purification in small scale. The recombinant monoclonal antibodies were further characterized for binding and their sequence analyzed, confirming the human nature of their VH and VK sequences. The selected hits were tested for their potential to interfere with the BMP9-mediated SMAD-1 phosphorylation, as the SMADs are key transmitters of the BMP9 signal.

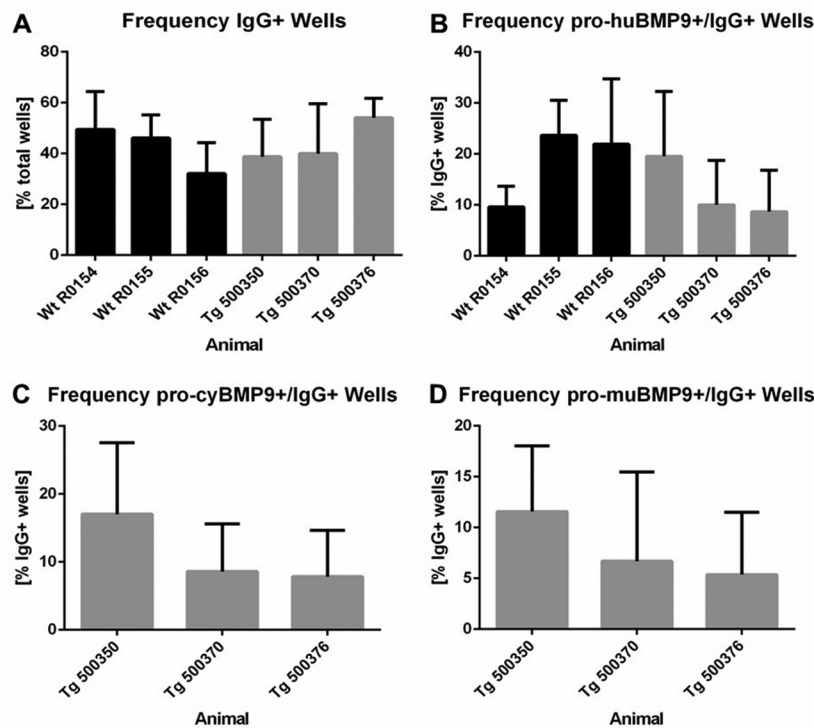


**Figure 4.** Yield of IgG-secreting and antigen-specific B-cell clones after primary screening. (a) Frequency of IgG-producing B-cell clones per total wells and (b) frequency of human BMP9-binding and IgG-secreting B-cell clones per total wells from wild-type and transgenic rabbits. Frequency of cynomolgus (c) or murine (d) BMP9-binding and IgG-producing B-cell clones per total wells from transgenic rabbits. For each parameter around 3500 wells were analyzed. The error bars represent the standard deviation. The lower cut off value of IgG-positive wells was  $> 0.013 \mu\text{g/ml}$  IgG and varied between OD 0.110 and OD 0.550 for BMP9-positive wells depending on the ELISA assay.

Using a specific pSMAD-1 (Ser463/465) assay, 56 fully human antibodies were identified displaying inhibitory activity on ALK1-positive immortalized endothelial EA.hy926 cells in response to BMP9 stimulation (Figure 5(a), correlation plot of pSMAD1 inhibition versus BMP9 binding). Moreover, almost 80% of those binders were confirmed to be triple reactive to human/cynomolgus/murine BMP9, the remaining 20% displaying cross-reactivity only to cynomolgus (data not shown).

One representative clone (in Figure 5(a) represented by the ring) with high potency was further tested in a dose-response curve as illustrated in Figure 5(b), confirming IC<sub>50</sub> in the nM range.

### Binding studies using surface plasmon resonance

The selected hits were analyzed for binding to pro-BMP9 by Biacore to ascertain whether high potency in the pSMAD1 assay correlates with high binding affinity. In order to minimize the risk of having avidity measured instead of affinity, 58 antigen-binding fragments (Fabs) were generated from the selected anti-BMP9 antibodies, comprising 55 pSMAD1 inhibitory and 3 non-inhibitory hits (BMP9.312, 335 and 353, see Figure 6) deriving either from the second or third immunization blood samples (Bleed 2 and 3). They were captured by anti-human Fab antibody directly immobilized on CM3 sensor chips.

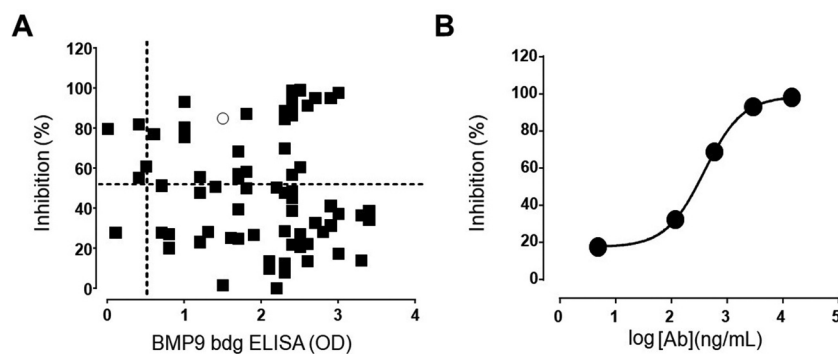


**Figure 5.** (a) Correlation plot single dose BMP9-binding ELISA versus SMAD1 inhibition assay. Only antibodies with binding results  $> 0.5$  (optical density) and inhibition  $> 50\%$  were selected for further evaluation. (b) Phospho-SMAD1-based IC<sub>50</sub> analysis of a representative anti-BMP9 antibody shows inhibitory potency in the nM range.

The BIAevaluation software allowed the analysis of maximum analyte binding capacity (called  $R_{max}$ ), which in this assay setup theoretically corresponds to saturation of all captured anti-BMP9 Fab molecules by one analyte molecule (human BMP9 pro-domain). The experimentally obtained  $R_{max}$  value can be set in relation to the expected  $R_{max}$  value (saturation response) and expressed as ratio  $R_{max}$  in percentage, where 100% is rarely achieved in reality. Slightly lower or higher values can be explained by partially mis-folded components (decreasing maximally achievable R-value) or potential unspecific binding (increasing the maximally achieved R-value), respectively.

The ratio  $R_{max}$  values for the anti-BMP9 interaction were determined to be between 0 and 258% (Figure 6). Of the selected Fabs, 52% showed binding of human BMP9 pro-domain in good agreement with the pSMAD1 inhibition assay as indicated by ratio  $R_{max}$  values between 60 and 145% in Figure 6, and by the high affinities ranking from nM to sub-pM KD range (data not shown).

Interestingly, Fab 282 showed a comparatively high Ratio  $R_{max}$ . As shown by Kienast et al.,<sup>12</sup> the pro-domains are released by an intramolecular shuffling during the binding of the BMP9 pro-domain to anti-BMP9 antibodies, implying that the target of the binding corresponds to mature BMP9. Calculating the Ratio  $R_{max}$  of the Fab 282 with the molecular mass of the BMP9 pro-domain, a value of 99% or 136% could be obtained for the human BMP9 pro-domain complex or the separate pro-domain, respectively, suggesting that the pro-domain might be the protein antigen specifically recognized by Fab 282. We then confirmed that Fab 282 does not bind the mature BMP9, strengthening the hypothesis that binder 282 is exclusively a pro-domain specific binder.

For detailed analysis, 14 surface plasmon resonance (SPR) binding positive Fabs and two negative controls, were selected to evaluate their kinetic binding properties and epitope groups. For estimation of the detailed kinetic binding properties, the selected Fabs were captured by anti-human Fab capture antibody directly immobilized on CM3 sensor chips. After evaluation of the obtained binding curves with the Langmuir 1:1 model ( $RI = 0$ ), the fitting curves showed deviations from the

apparent binding curves to various extents, suggesting that more than one binding event could occur (Figure 7(a)). Binding curves were then analyzed using the Interaction Map® software of Ridgeview Diagnostics AB, which confirmed the existence of more than one binding event (Figure 7(b)). The binding parameters generated by the BiaEvaluation software taking into account the additional binding event (see Table 4), confirmed the previously determined broad range from nM to sub-pM KD, highlighting the potential of the transgenic rabbits to generate very high-affinity antibodies. For 11 of the 14 clones, a double-digit picomolar affinity or even higher could be confirmed by using the Interaction Map software.

For epitope binning analysis, the preincubated complex of Fab and BMP9 pro-domain was injected to the Fab that was captured by the directly immobilized anti-hFab antibody on the CM3 sensor chip. To avoid undesired binding of the pre-complexed Fab molecules, free binding sites of the capture antibody were blocked. Then, the relative normalized binding of the Fab:BMP9 pro-domain complex was compared to the relative normalized binding of BMP9 pro-domain alone and calculated as binding ratio. Thirteen Fabs with sufficient binding response were analyzed for their epitope binning properties using a hierarchical clustering method as described in Materials and Methods. These belonged to three different epitope groups (bins), as shown in Figure 8.

The binders displayed a broad range of binding kinetics within a given bin, including very high-affinity antibodies. Figure 9 illustrates the diversity of the obtained binders at affinity and epitope levels. The sequence diversity (concatenated complementarity-determining regions (CDRs) from VH and VK sequences) of the binders is highlighted later in Figure 13 (Sequence Diversity session) and in Supplementary material, Fig. 20 (Part 10).

### Sequence analysis of antigen-specific antibodies

Sequence analysis of the 107 primary hits revealed that 82% of the selected hits delivered antibodies with fully human VH and VK domains. The remaining 18% were chimeric antibodies

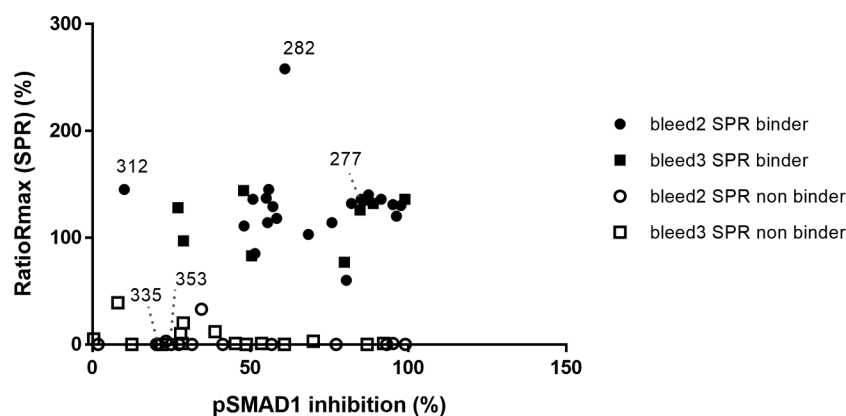


**Figure 6.** Correlation of the pSMAD1 inhibition with binding of BMP9 pro-domain using SPR measurements. Full and empty dot/quads indicate SPR binders and non-binders respectively, derived either from the second (dot) or the third (quad) immunization blood samples (Bleed 2 and 3). Bmp9.312, 335 and 353 are 3 non-inhibitory hits selected as reference.

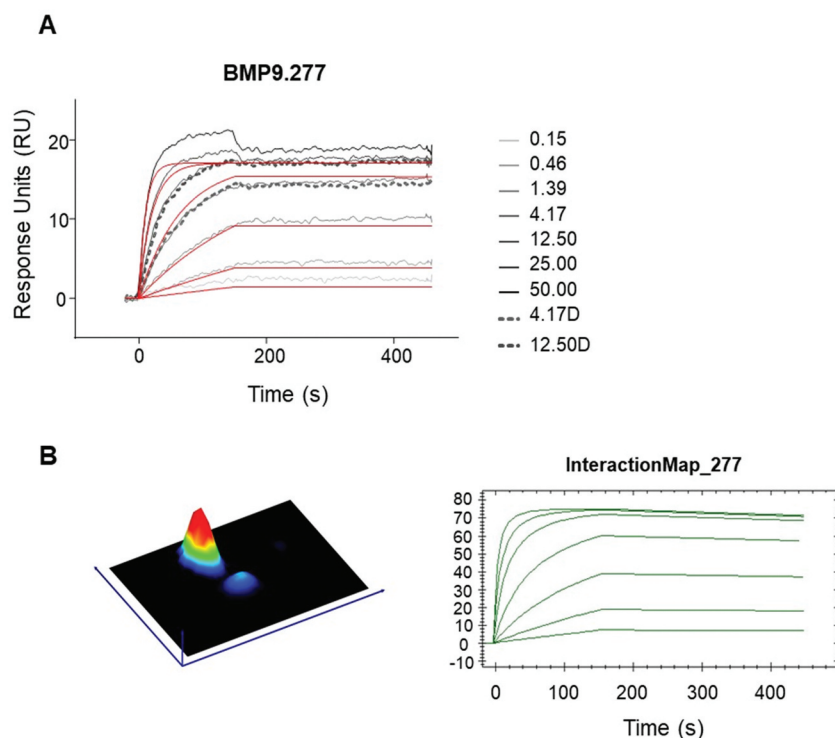


**Figure 7.** Detailed kinetic analysis of obtained binding curves using surface plasmon resonance, where the anti-human BMP9 Fab molecules were captured to chip surface via anti-human Fab capture antibody and the binding of the human BMP9 pro-domain was analyzed. The obtained binding curves were evaluated using (a) the B4000 BiaEvaluation software, where the black lines corresponds to the measured binding responses and the red lines to the fitting curves using Langmuir 1:1 fit model with RI = 0 and (b) the InteractionMap® of Ridgeview Diagnostics Ab.

**Table 4.** Kinetic interaction parameters of human BMP9 pro-domain and anti-BMP9 Fab molecules. Association ( $k_a$ ) and dissociation ( $k_d$ ) rate constants, and the resulting dissociation equilibrium constants  $K_D$  as determined by B4000 BIAevaluation Software using a 1:1 Langmuir fit.  $K_D$  values represent avidity in addition to affinity binding due to possible bivalent binding of dimeric BMP9 to the two captured Fab molecules. Ratio Rmax is calculated for mature human BMP9 after release of pro-domain. Some of the obtained kinetic parameters are evaluated by the software but marked because they are outside of the limit of instrument (red labels).

Fab	Ratio Rmax (%)	Rmax (RU)	$k_a$ (1/Ms)	$k_d$ (1/s)	$K_D$ (pM)
Bmp9.276	79	9	3.1E+07	3.73-03	119
Bmp9.277	124	18	3.6E+06	5.1E-07	0.1
Bmp9.279	122	11	2.4E+07	1.5E-06	0.1
Bmp9.280	123	12	3.0E+07	1.0E-03	34
Bmp9.282	366	22	5.3E+05	1.5E-03	2904
Bmp9.284	140	13	3.6E+06	3.8E-05	11
Bmp9.286	130	4	5.1E+06	3.3E-04	65
Bmp9.288	95	14	1.2E+06	1.5E-07	0.1
Bmp9.289	125	16	8.5E+06	1.6E-06	0.2
Bmp9.290	120	15	3.3E+07	4.5E-04	14
Bmp9.305	114	15	9.7E+06	9.7E-06	1
Bmp9.306	78	14	1.9E+07	2.4E-06	0.1
Bmp9.312	131	12	2.9E+06	6.2E-04	214
Bmp9.314	41	8	1.4E+06	1.5E-06	1

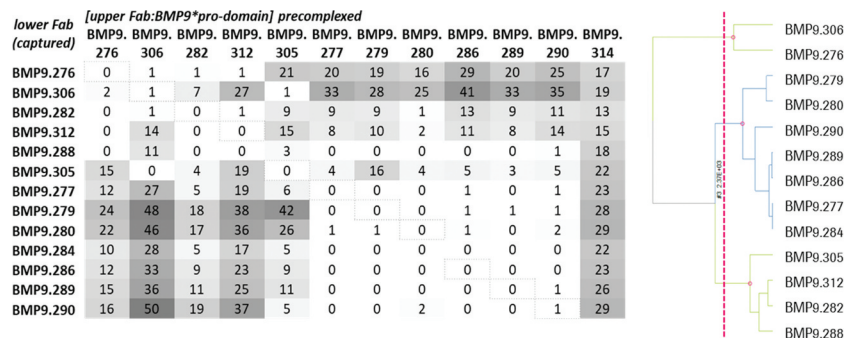


**Figure 8.** Epitope binning analysis using SPR. The upper Fab was precomplexed with a 20fold molar excess of BMP9 pro-domain and then the binding to the captured Fab was analyzed. The values correspond to the ratio binding (%) calculated from the normalized binding of the Fab:BMP9 complex divided by the normalized binding response of the BMP9 pro-domain alone.

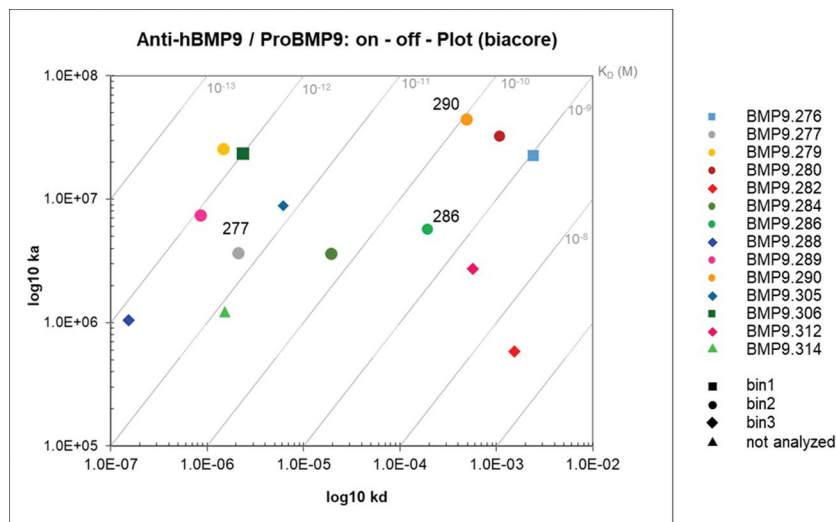


**Figure 9.**  $K_{on}/K_{off}$  plot – epitope bins of selected hits. Highlighted were the antibodies according to their respective epitope bins analyzed by SPR.

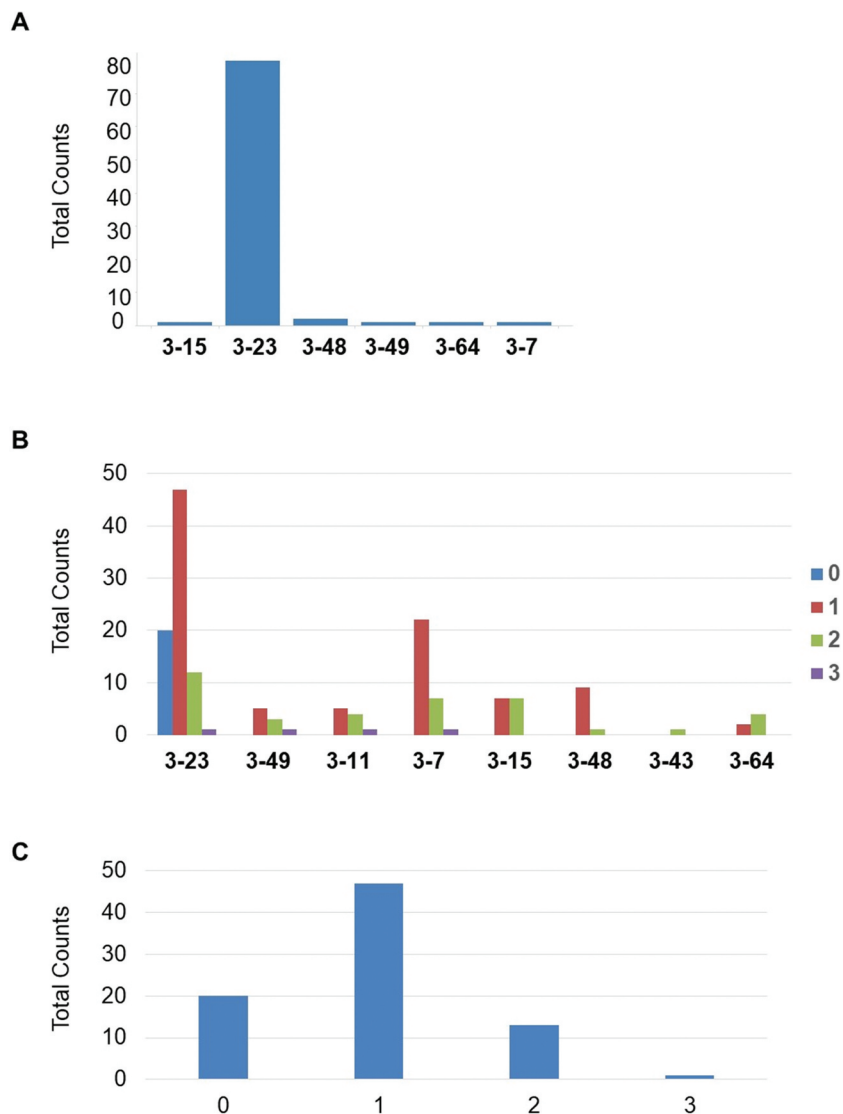


**Figure 10.** (a) Involvement of integrated V3 germlines in VDJ rearrangement. (b) Involvement of the 8 transgenic human germline VH sequences within the GC events. (c) Whole number of GC events in the BMP9 specific human heavy chain variable regions.

with an rbVH-huVK combination binding BMP9 and occurring despite the knockout of the rabbit IgM gene in the transgenic strains. Interestingly, 83% of these rbVH-huVK sequences contained a human JH (15/18) and only 3 of 18 sequences contained a rabbit JH. Only fully human, non-redundant antibodies (in total 81) were further analyzed for germline usage, GC, humanness, maturation and Heavy Chain (HC) CDR3 diversity.

### Analysis of Gene Conversion, Germline Usage and Mutation Rate

We next commenced to analyze in more detail the diversity at the sequence level of the antigen-specific repertoire including the underlying maturation mechanisms like gene rearrangements, GC and somatic hypermutation. The DNA sequences of the V-elements of all human antigen-specific antibodies were compared to the best matching region of the integrated V germlines for germline usage analysis (V-elements involved in VDJ-VJ rearrangements for the heavy and light chain, respectively). Thereby, the mutation rate was also evaluated and the heavy-chain variable domains were manually scrutinized for involvement in likely significant GC events. Though we found many very significant GC events, we have to note that some events were judgment calls based on expert knowledge as the eight VH3 germlines are so closely related that in some sequences we lacked sufficiently distinct markers that differentiate the germline-like sequence fingerprints. An example of a GC event and the evaluation criteria are shown in Supplementary material, Part 10, Fig. 21. It illustrates a clone with two very significant GC events causing three different human germlines to be involved. The path through the

sequence is marked by inverse black. The presumable basic germline VH3-23 is almost lost due to two alternative human germlines (VH3-15 and VH3-49) crossed in at the N-terminal (3–15) and main part (3–49) of the V-region.

As shown in Figure 10(a), all of the 8 human VH3 germlines are involved in the VDJ rearrangements, the most frequently used is the VH3-23, the most proximal V germline to the J segments in the integrated construct. VH3-23 is also the most common VH3 element in human antibody repertoire.<sup>16</sup> By GC analysis, we demonstrated the involvement of all integrated VH3 germlines in the calculated GC events (up to three events recorded for a given VH) (Figure 10(b)) with a tendency of greater usage of those in the middle of the transgenic VH locus. About 75% of the clones show at least one GC event, whereas one clone has 3 such events (Figure 10(c)).

Interestingly, at the beginning of the screening cascade, those clones without any significant gene-conversion event represent a quarter of all antigen-specific antibodies (Supplementary material, Part 10, Fig. 22). Their frequency along the screening chain converts to 46% among clones not further selected after primary screening, and to 0% among clones selected after functional assay.

We further looked at the impact of GC on mutation rate on both the CDR and FR (Framework Region) regions as illustrated in Figure 11(a,b). The DNA mutation rate in percentage compared to the reference best matching human germline was calculated for all CDRs and FRs of the BMP9 human binders (Figure 11(a)). The mutation rate was significantly higher in the CDR than the FR regions. In CDR2, the mutation rate is clearly increased for sequences having undergone 3 GC events, demonstrating the contribution of this mechanism to sequence diversity in addition to somatic hypermutation. In reverse, GC

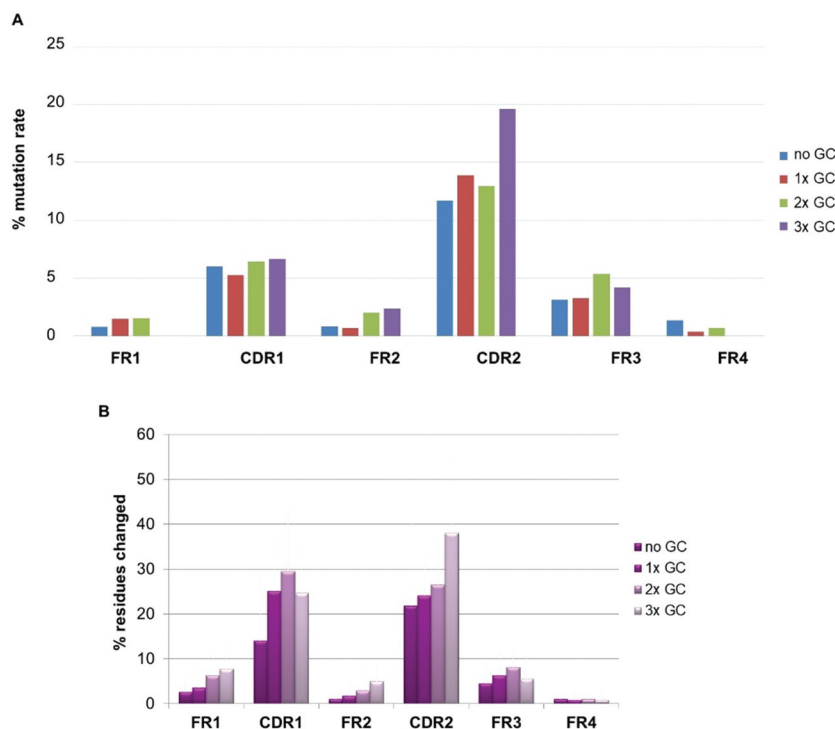


**Figure 11.** (a) Percentage of DNA mutation rate in CDRs and FRs of antibodies binding to BMP9; (b) Percentage of protein mutation rate in CDRs and FRs of about 1700 antigens specific antibodies from 10 different immunization campaigns.

does not increase the mutation rate in the FR regions. To confirm the result, a quite comparable distribution was observed when a similar analysis was performed (on protein level) on 1700 human antigen-specific binders from 10 different immunization campaign (ca. 30 transgenic rabbits) (Figure 11(b)).

Germline Usage and mutation rate analysis for the light chain are delivered in Supplementary material, Part 10, Fig. 23–24.

### Analysis of humanness

We are aware that the definition and the method of evaluation of the “degree of humanness” of a therapeutic antibody are still a matter of debate,<sup>17</sup> but nevertheless we investigated the degree of humanness of the fully human antigen-specific antibodies by measuring the percentage of homology of V and V + J elements to the best matching human germline for both heavy and light chain at the protein level (Figure 12(a,b)).

For the heavy and light chain, over 95% of all antibody sequences show a homology to a single human germline V-element larger than 85% (the cutoff of homology defined by the American Medical Association required for an antibody to be considered as “human”). This was also observed for the 56 fully human antibodies displaying inhibitory activity (data not shown). A set of commercial antibodies (Supplementary material, Part 10, Fig. 25) was similarly analyzed with two in-house-developed approaches and with the method described by Abhinandan and Martin,<sup>18</sup> and they exhibited a degree of

humanness comparable to the in-house generated BMP9 antibodies. Having shown that GC mainly occurs in the CDRs, we demonstrate here that this does not lead to a reduction in the humanness of the selected antibodies.

D elements are specifically involved in the junctional diversity process arising when the fusion of V, D, and J segments is not exact. Such “imprecise joining” of gene segments can result from the deletion of nucleotides in the joint region, and/or the addition of P and/or N nucleotides during V(D)J recombination, and leads to the high variability of HC-CDR3 sequences. As the D elements in transgenic rabbits are not humanized, we wanted to investigate if the rabbit origin of D elements in HC-CDR3s from transgenic rabbits human antibodies could still be recognized. We analyzed a dataset of over 900 HC-CDR3 amino acids sequences from transgenic rabbit monoclonal antibodies, isolated from several animals and several in-house (Roche) projects and, as reference, over 5000 human HC-CDR3s selected by annotation from the IMGT database. Each single HC-CDR3 sequence was run against the human and the rabbit D-element collections by the homology search application FASTA and the top score collected as a measure for the fit of the best match. Details on the method and scores distribution are provided in Supplementary material (Fig. 26, Part 10). The distribution of HC-CDR3s scores vs D-elements shows that the majority of HC-CDR3 sequences (over 90%) cannot be assigned to their respective human or rabbit origin. Only a small fraction (<15%) of rabbit transgenic HC-CDR3s score better against rabbit D-elements, and a similar portion of human HC-CDR3s score better against

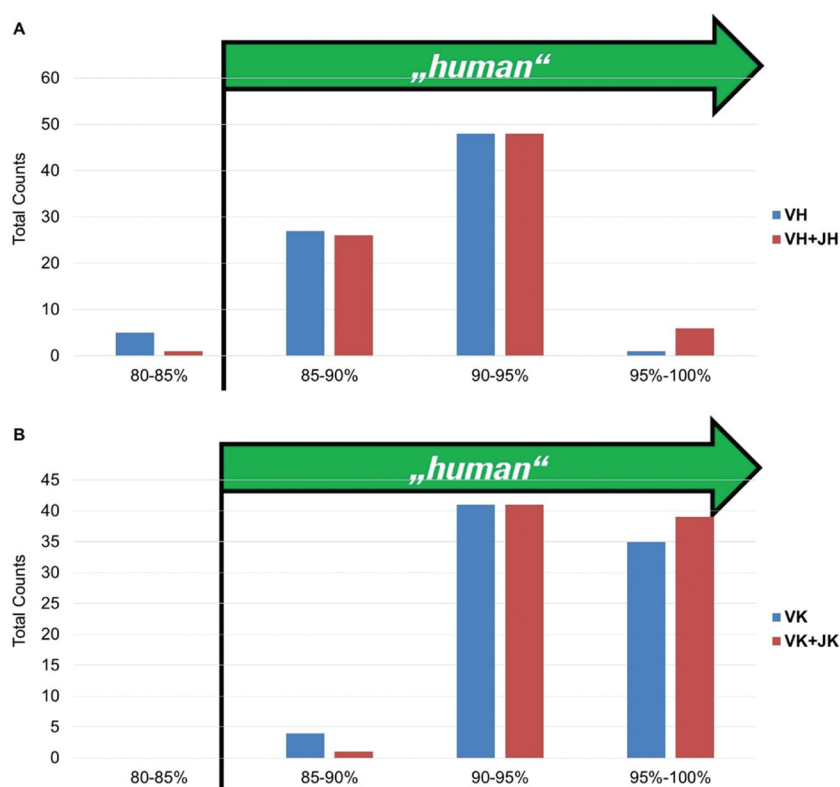


**Figure 12.** “Humanness” of fully human BMP9-specific binders compared to the best matching human VH (a) and VK (b) germlines. The 85% cut off corresponds to the percentage of homology defined by the American Medical Association (AMA) required for an antibody to be considered as “human”.



counterparts, and moreover the human/chimeric IgM and IgG serum titers were comparable as well. This shows that the transgenes did not affect the ability of the rabbit B cells to survive and proliferate, confirming that: 1) the vector design, and 2) the expression strategy enabled successful cell-surface expression and signaling capability of the human B cell receptor on transgenic rabbit B cells.

Several regulatory elements in immunoglobulin genes have been described. In particular, the enhancers downstream of the heavy-chain constant region and intronic enhancers in light chain genes<sup>20–24</sup> are extremely important. Studies in mice have shown that the membrane and cytoplasmic tail of membrane-bound immunoglobulins play an important role in expression levels of human-mouse chimeric antibodies in mice transgenic for the human C $\gamma$ 1 gene.<sup>25</sup> JH germline mutant mice producing human immunoglobulins have been described, indeed expressing only low levels of human antibodies, probably due to the lack of species-specific regulatory elements in the immunoglobulin loci that are necessary for efficient expression of immunoglobulins.<sup>26</sup> Moreover, we expected that especially in animals that diversify their primary antibody repertoire by mainly GC and hypermutation (additionally to gene rearrangement),<sup>27</sup> a set of animal-specific regulatory mechanisms are used. For these reasons, rabbit/human chimeric transgenic vectors have been generated containing humanized immunoglobulin loci flanked by endogenous regulatory and antibody production machinery from the non-human, gene-converting species, mainly rabbit and chicken (as with rabbits, chicken also uses a GALT-driven B-cell repertoire).<sup>28</sup>

Furthermore, for B-cell survival and B-cell maturation, a functional B-cell receptor consisting of the cell-surface IgM and the adjacent CD79a and CD79b is crucial.<sup>28,29</sup> Combining 1) the abrogation of the endogenous B-cell repertoire by knockout of the rabbit IgM, 2) the introduction of human CD79a/b, and 3) the co-transcription of human Bcl2, we pushed the level of B cell survival and maturation<sup>30,31</sup> to the levels of the B-cell repertoire of wild-type rabbits. The final transgenic rabbit strain is transgenic for human IgG VH3 and VK1 family genes, human JH/K locus, human CD79a/b as well as Bcl-2, showing a wild-type like humoral and B-cell immune response. Unexpectedly, we observed that a majority of clones still carried a rabbit constant domain, despite the lack of rabbit IgM in the rabbit IgM knock-out rabbits. This does not preclude the use of the strain for antibody generation, as the Fc part of an antibody can be easily exchanged recombinantly. Although to date we have not elucidated the mechanism, possible explanations include cis-recombination and interallelic class-switch recombination, which might point to a selection pressure of a particular immunological checkpoint at the IgG Fc part during the rabbit B-cell cycle.<sup>32–39</sup>

The analysis of the VDJ sequence in the transgenic rabbits revealed that approximately 82% of all sequences are correctly joined together, delivering a human huVH-D-huJH sequence. In matured IgG antibodies, the original rabbit-derived DH sequence is highly altered and quite antibody-specific so that it can hardly be assigned to a specific rabbit (or human) DH germline sequence. Remarkably, 18% of all analyzed VDJ sequences still displayed a rabbit VH, mostly joined by a human JH (83%), pointing to a recombination event in the

DH-gene segment. This is in line with the literature describing recombination events downstream of VH genes and upstream of JH<sup>33,40</sup> as a rare phenomenon during generation of rabbit VDJ sequences.

Diversification of the variable gene regions by somatic hypermutation, and more importantly by GC, was found in the majority of the selected clones. The overall DNA mutation rate was significantly higher in the CDR than the FR regions for both light and heavy chain, which is in line with the literature. As observed from VH sequence analysis, all of the integrated human VH were used in GC, yielding a considerable increase of the mutation rate in the CDR regions, while not particularly affecting the diversity of the framework regions. Similar results have been observed also in transgenic chicken carrying immunoglobulin gene,<sup>41–43</sup> and this may be due to the high homology of the VH gene segments in their FR, or possibly also on the main role of the CDR in the *in vivo* antibody selection process.

The frequency of GC events increased after selection for higher affinity, potency, and function, and most importantly, it did not lead to a reduction in the humanness of the isolated antibody sequences, a pivotal aspect for drug development. Much more data will be needed to ascertain whether there is a relationship between frequency of GC events and antibody-positive selection, for which we could not rule out an antigen-specific component at this stage. Our observation, however, is entirely compatible with GC being an important mechanism of the generation of diversity and of the affinity maturation process<sup>44–46</sup> in the rabbits transgenic for human immunoglobulin genes.

Due to the high complexity of the analysis dealing with 29 VK segments as donors for GC, GC data for the light chains are not yet available. Current efforts for scrutinizing GC events in an automated way should give us a deeper overview of the impact of GC in the maturation of the human transgenic light chains in the future.

The diverse set of antibodies generated led to the identification of numerous functional antibodies inhibiting BMP9 as shown by the pSMAD assay. These antibodies recognized multiple epitopes and were cross-reactive to the homologous BMP9 protein of cynomolgus macaque and mouse. The antibodies covered a wide range of affinities, including very high-affinity clones. We are fully aware that the highest affinity values obtained are at the limit of resolution of the Biacore technology. Therefore, we used Fabs together with very low protein densities on the sensor chips to minimize the risk of measuring avidity instead of affinity, and deconvoluted what appeared to be an additional binding event. This more precise investigation of the binding curves confirmed the measured affinities, which were also in line with the potency of the clones determined in the pSMAD assay.

In addition, we note that high affinity is only a proxy for evaluating the performance of the strain. For a number of applications and when functional assays are used early in the screening tree, such as for agonist antibodies, the diversity of the repertoire and the resulting function of the antibodies is what primarily matters. Those cases currently comprise a substantial proportion of antibody discovery projects. This notwithstanding, we have generated further examples of antibodies for which high affinity was expected as a property resulting from the selection process, as shown in Supplementary material, Part 10, Fig. 27.

In summary, we have demonstrated in this work that the antibody diversification mechanisms at play in rabbits can be made to work on human transgenic immunoglobulin gene segments, leading to the generation of a diverse set of functional and very high affine human antibodies. Furthermore, we show that the GC mechanism uses all transgenic human VHs and is associated with a higher mutation rate in the CDR regions. We detected up to three GC events in the heavy chain. As an outcome, this diversification mechanism enhanced the transgenic human antibody sequence diversity without compromising the human character of the generated antibodies, thereby delivering very specific and highly affine BMP9-inhibiting human antibodies.

## Materials and methods

### Construction of modified human IgG loci using bacterial artificial chromosomes

The transgenic immunoglobulin heavy and light chain constructs were intended to generate transgenic rabbits expressing humanized antibodies. The transgenic vectors contain humanized immunoglobulin loci, while leaving the endogenous regulatory and antibody production machinery of the non-human animals essentially intact. Rationale and details on construction are described in Patent Number US RE47, 131 E, US 835456B2 and on Supplementary material (Part 1, Fig. 14–18).

### Microinjection and embryo transfer

All animal procedures were approved by the Government of Upper Bavaria (permit numbers 55.2-1-54-2531-26-04, 55.2-1-54-2531-9-09, and 55.2-1-54-2532-76-09) and performed according to the European Union Normative for Care and Use of Experimental Animals. Details on microinjection and embryo transfer procedures are included in Supplementary material, Part 2.

### Analysis of transgenic founders and lines

The integration of the different transgenic human regions was verified by PCR analysis. The numbers of integrated FHHC1.1-bcl2 and FHL1.1 transgene copies were determined as Comparative  $C_T$  experiments on an ABI Prism 7500 Real-Time PCR system in comparison to the endogenous rabbit C-gamma and C-kappa loci (2 copies per genome) using Universal ROX-Mix reagent (Roche) according to the instructions by the manufacturers. Primers, probes, and PCR conditions for the different PCR assays are indicated in Table 6 in Supplementary material, Part 4.

Fluorescent in situ hybridization was performed with chromosome preparations derived from peripheral blood cells of transgenic rabbits (at least two animals from each line), by an external service provider, Chrombios GmbH (Nussdorf am Inn), according to their standard procedures. Each preparation was analyzed with two fluorescently labeled BAC-derived probes, one for the wild-type locus and one for the transgene. For each preparation, approximately 10 metaphases were evaluated.

### Breeding and genotype specifications

Rabbits were bred and maintained in an American Association for Accreditation of Laboratory Animal Care International-accredited facility under specific pathogen-free conditions. Starting from founding animals, rabbits were bred to successively combine all transgenic and knockout loci.

- (1) rbIgM KO x rbIgK KO (Basilea mutation<sup>13</sup>)
- (2) huIgG x huIgK
- (3) huIgG/huIgK x rbIgM KO/rbIgK KO
- (4) huIgG/huIgK/rbIgM KO/rbIgK KO x huCD79a/b

Immunized rabbits were hemizygous ( $\pm$ ) or homozygous (+/+) for huIgG transgene, homozygous (+/+) for huCD79a/b and huIgK and homozygous or compound heterozygous for rbIgM KO (Table 1).

Details on husbandry conditions and breeding, Parents and Predecessors of immunized rabbits are provided in Supplementary material, Part 5, Table 7–8.

### Cloning and purification of recombinant BMP9 variants and pro-domain

Cloning, expression, and purification of BMP9 pro-domain (amino acids 23–319) and mature protein (amino acids 320–429) were performed at Roche Innovation Center Munich as described previously.<sup>11,12</sup> The pro-BMP9 gene is rather conserved in several species. The identity of the amino acid sequence of human and cynomolgus pro-BMP9 is 96.1% and of human and mouse pro-BMP9 is 81.8%.

### Serum analytics of transgenic rabbits

Antibodies, reagents, and conditions used for ELISA IgM and IgG serum analytics are described in Supplementary material, Part 6, Table 9. For antigen-specific serum titers analysis, human BMP9 pro-domain was immobilized on a 96-well NUNC Maxisorp plate at 2.5  $\mu$ g/ml. Antisera, were serially diluted in 0.5% Crotein C in Phosphate-buffered Saline (PBS), 100  $\mu$ l/well; detection was performed with one of the following reagents: 1) horseradish peroxidase (HRP)-conjugated donkey anti-rabbit IgG antibody (Jackson ImmunoResearch/Dianova 711-036-152; 1/16 000); 2) HRP-conjugated rabbit anti-human IgG antibody (Pierce/Thermo Scientific 31423; 1/5000); or 3) biotinylated goat anti-human kappa antibody (Southern Biotech/Biozol 2063-08, 1/5 000) and streptavidin-HRP, each diluted in 0.5% Crotein C in PBS, 100  $\mu$ l/well. Titer was defined as dilution of antisera resulting in half-maximal signal.

### Immunization

3 New Zealand White rabbits and 3 transgenic rabbits were immunized at day 0 (by intradermal application) with 400  $\mu$ g and at days 7, 14, 42, 70, and 98 (by alternating intramuscular and subcutaneous applications) with 200  $\mu$ g of a recombinant human BMP9 pro-domain preparation, emulsified with complete Freund's adjuvant. Blood (10% of estimated total blood

volume) was taken at days 20, 48, 76, and 104 for serum preparation and peripheral mononuclear cells isolation.

### **Isolation, immune fluorescence staining and flow cytometry of PBMC**

PBMCs were isolated from ethylenediaminetetraacetic acid-containing blood samples following instructions described previously.<sup>15</sup> After depletion of macrophages and monocytes, cell suspensions from immunized animals were further enriched on sterile cell culture 6-well plates coated with 2 µg/ml of human BMP9 pro-domain protein following the panning procedure specified in Seeber et al.<sup>15</sup>

For the pre-immune FACS analysis, the anti-rabbit IgG Fc antibody Fluorescein Isothiocyanate (FITC)-labeled and the anti-human CD79a antibody (A488) were from AbD Serotec. The phycoerythrin (PE)-labeled anti-rabbit IgM was purchased from BD Pharmingen (624048). The PE-labeled anti-human CD79b antibody (335833) and the allophycocyanin-labeled anti-human IgG1 antibody (550931) were purchased from BD Biosciences. The anti-human IgM antibody (FITC) was from Biolegend (314506). The anti-human light chain antibody (PE) and the DyLight488-labeled anti-human IgG1 Fab were ordered from Dianova (109-486-170).

B cells retrieved from immunized animals were single-cell sorted as previously described<sup>15</sup> using the FITC-labeled anti-rabbit IgG from AbD Serotec (STAR121F). With this antibody human IgG1 Fc- as well as rabbit IgG Fc-positive B-cells could be detected, implying that this polyclonal anti-rbIgG-Fc antibody is cross-reactive to the cell surface-expressed human IgG1 Fc. However, staining intensity of huIgG Fc and rbIgG Fc was different, allowing for differentiation of huIgG and rbIgG-positive B cells.

### **B-cell cultivation and IgG quantification**

The B-cell cultivation was performed as described in Seeber et al.<sup>15</sup> The supernatants of B-cell cultivation were used for screening assays. The quality of the B-cell cloning process was assessed by the frequency of IgG-secreting B-cell clones (% total wells: all deposited B cells) and by the frequency of B-cell clones secreting antigen-specific monoclonal antibodies (% IgG-positive wells). After the removal of the supernatants, the remaining cells of the B-cell clones were lysed by 100 µl RLT buffer (Qiagen, Hilden, Germany) and stored in DNA LoBind 96-well deepwell plates (Eppendorf, Hamburg, Germany) at -20°C for RNA preparation. For the quantification of the IgG, a rabbit Fc-specific ELISA was performed as described in Seeber et al.<sup>15</sup> ELISAs detecting human IgG were not conducted since we experienced a very low frequency of transgenic B cells displaying IgG with human Fc over the course of the analysis of the transgenic rabbits (data not shown).

### **Antigen-binding immunoassays and statistical calculations**

The antigen-binding assay was performed by ELISA at room temperature (RT) on 384-well Maxisorp plates (ThermoScientific) coated overnight at 4°C with 100 ng/

ml recombinant human/cynomolgus or 200 ng/ml recombinant murine BMP9 pro-domain complex diluted with PBS buffer. Detection was with IgG conjugated with HRP (Amersham, #NA9340) at 1:4000 in PBST (PBS + 0.05% Tween 20) + 1% bovine serum albumin (BSA) for 1 hr. For the determination of the cut-off values of positive antigen binders after primary screening, we used a robust quartile-based method for outlier detection.<sup>47</sup> The method uses the median as an estimate for the center of a given data set. The spread of the data set is estimated by the interquartile range (IQR) divided by 1.34898, which is akin to one standard deviation if the data is normally distributed. We define as outliers all data points that are greater than median plus 3x spread. All calculations were performed with the software JMP 10 (SAS Institute GmbH, Böblingen, Germany). After secondary screening, all EC50 were calculated using a four-parameter logistic model from GraphPad Prism 5.0.

### **PCR amplification of cognate VH and VK**

Total RNA preparation from B cells lysate (resuspended in RLT buffer – Qiagen – Cat. N° 79216) and cDNA synthesis were performed as described previously.<sup>15</sup> The cDNA of the immunoglobulin heavy and light chain variable regions (VH and VK) was amplified with the AccuPrime Supermix (Invitrogen 12344-040) using the primer pairs rbHC.up and rbHC.do for the heavy chain (rabbit Fc) and BcPCR\_FHLC\_leader.fw and BcPCR\_huCkappa.rev for the light chains (human C kappa). The primers and PCR conditions are provided in Supplementary material Table 10, Part 8. All forward primers were specific for the signal peptide (of respectively VH and VK), whereas the reverse primers were specific for the constant regions (of respectively VH and VK). PCR products were purified using the NucleoSpin Extract II kit (Macherey&Nagel; 740609250) according to manufacturer's protocol.

### **Recombinant expression of monoclonal bivalent antibodies**

For recombinant expression of monoclonal bivalent antibodies, PCR-products coding for VH or VK were cloned as cDNA into expression vectors by the overhang cloning method<sup>48,49</sup> and transiently co-transfected into HEK293 cells as described in Seeber et al.<sup>15</sup> Three variants of the basic expression plasmid were used: one plasmid contained the rabbit IgG constant region designed to accept the VH regions, a second plasmid contained a truncated (CH1-Hinge) rabbit IgG constant region designed to accept the VH regions in the Fabs, and finally a third plasmid contained a human kappa-1 LC constant region to accept the VK regions. After purification by Protein A column standard protocols, supernatants were further analyzed for antibody content and specificity.

### **High Throughput Screening**

During screening, CyBio Well vario pipettors (Analyticjena) were used for all plate-to-plate liquid transfers. Wash steps and

liquid additions were carried out using Matrix WellMate™ devices (ThermoFisher). The final optical density read was performed using EnVision Multimode Plate Reader (PerkinElmer). All devices were part of a CyBio® Screen-machine automation platform. Data management and visualization was supported using Tibco Spotfire data visualization and analytics software (PerkinElmer).

### **Phospho-SMAD1(Ser463/465) assay**

The anti-BMP9 antibody-mediated inhibition effect on the pSMAD pathway was determined by quantification of the pSMAD Ser463/465 phosphorylation in human endothelial cell using a phospho-SMAD1(Ser463/465) Terbium SureFire Ultra Detection (PerkinElmer). Briefly, 55x10(6) EAHy926 cells were seeded in a well of a 384 w culture plate in 30  $\mu$ l RPMI1640 and 0.5% FCS (Fetal Calf Serum. After 21 h cultivation in RPMI culture media, buffer was changed to 30  $\mu$ l 1xHBSS/20 mM HEPES/1xPBS at RT (20 min) and incubated with increasing concentrations of anti-BMP9 antibodies in a volume of 5  $\mu$ l and 5  $\mu$ l 2.5 ng/ml BMP9 for 2 h at 37°C/5% CO<sub>2</sub>. The cells were treated with 25  $\mu$ l lysis buffer (PerkinElmer) for 45 min at RT. The 20  $\mu$ l volume was transferred to a 384 w assay plate (PerkinElmer) to enable the detection of pSMAD (Ser463/465). pSMAD was quantified by consecutively adding 5  $\mu$ l acceptor beads and 5  $\mu$ l donor beads. After 1 hr incubation, the emission read out at 520–620 nm was sampled using an EnVision Multimode Plate Reader (PerkinElmer). All IC<sub>50</sub> values were calculated using a four-parameter logistic model from GraphPad Prism 7.0.

### **Surface plasmon resonance**

All experiments were performed on Biacore B4000, T200 or 8 K instruments (GE Healthcare) in running buffer PBS containing 0.05% Tween at 25°C. Samples were diluted in running buffer containing 1 mg/ml BSA. When capture kits were used, the chip surfaces were regenerated as recommended by the vendor. Standard amine coupling procedures were carried out as recommended by the vendor (GE Healthcare) in HBS-N buffer (GE Healthcare BR-1003-69). For kinetic measurements  $\mu$ -purified transgenic rabbit Fab molecules were captured via human Fab Capture kit (GE Healthcare 28958325) using CM3 sensor chip (GE BR100536). Capture levels were adjusted to achieve a maximal analyte response of 30 response units. The analytes were injected as series with a dilution factor of three or 10 with an association phase of 150 s, followed by a dissociation phase of 300–900 s at a flow rate of 30 or 50  $\mu$ l/min. Data were evaluated with Biacore Evaluation software (B4000 version 1.1, T200 version 3.1, 8 K Insight Evaluation version 2.0.15.12933), including double referencing against blank and against reference flow cell containing no capture molecule. Kinetic constants were calculated from fitting to a 1:1 Langmuir binding model (RI = 0). The Ratio R<sub>max</sub> is defined as R<sub>max</sub> experimental/R<sub>max</sub> theoretical, where 100% theoretical response maximum is calculated from the capture level of the first interaction partner (as the Response Units are

directly proportional to molecular weight), assuming one binding sites for the dimeric BMP9. For detailed analysis of KD values, Interaction Map® software of Ridgeview Diagnostics AB was used.

### **Epitope binning**

For epitope binning analyses, Fab molecules were captured via human Fab Capture kit (GE Healthcare) using CM3 sensor chip. The BMP9 pro-domain complex was pre-incubated with a 20-fold concentration excess of transgenic rabbit Fab molecules. The binding of the Fabs was compared to the binding of BMP9 pro-domain complex alone (relative binding ratio value). To avoid back binding of the upper Fabs, free capture molecules were blocked with ChromPure human IgG, (Jackson ImmunoResearch 009–000-007).

The heat map and the bins were calculated using the hierarchical clustering method of the software Tibco spotfire. To determine the most probable number of binding modes, a table was generated with one row for each antibody. Columns represent competing antibodies and give the degree of binding affinity decreases by each competing antibody.

The rows in the table were then clustered with agglomerative hierarchical clustering. The optimal cluster count was determined through systematic evaluation of combinations of five agglomeration methods (average linkage, single linkage, complete linkage, Ward's method and weighted average linkage), five distance metrics (Euclidean, Manhattan, correlation, Squared Euclidean and Half Squared Euclidean) and all possible cluster counts (from two to the number of rows in the table). The best combination was determined with Silhouette scoring.<sup>50</sup>

### **Bioinformatic tools for sequence analysis**

For the bioinformatics sequence analysis, all clones were available as complete DNA sequences of the heavy and light chain variable regions. For the analysis of mutations in FR and CDR regions, we compared the DNA sequences of each of these regions to the best matching region of the eight human VH3 germlines. For the humanness analysis, we compared the complete protein sequences of the VH-elements  $\pm$  FR4 (J-element) to the best matching of all available human germlines. For all analysis, CDRs are defined as the superset of Kabat and Chothias definitions: according to Kabat H1 is 26–35B, H2 is 50–65, H3 is 95–102.

The DNA of all V-elements as part of the human variable regions were manually scrutinized for the most likely GC events by comparing the given sequence to the sequences of the eight human VH3 elements available in the transgenic rabbits. Consecutive stretches of none or comparable less deviations between a distinct germline and the given sequence of a clone were used to assign the most likely originating germline at a certain position. Yet there is no clear-cut rule to distinguish between an additional hypermutation in a germline and calling a GC of another germline that has no hypermutation at this position. We accepted only significant and highly likely GCs as such (shown in Supplement), but rejected questionable GCs. Thus, a certain degree of uncertainty remains due to this heuristic methodology.

## Abbreviations

ALK1	Activin receptor-Like Kinase 1
BAC	Bacterial Artificial Chromosomes
Bcl2	B-cell lymphoma 2
BMP9	Bone Morphogenetic Proteins 9
CDR	Complementarity-Determining Region
F2A	Self-cleaving peptide
FACS	Fluorescence-Activated Cell Sorting
FCS	Fetal Calf Serum
FHHC	Fully Human Heavy Chain
FHLC	Fully Human Light Chain
FITC	Fluorescein Isothiocyanate
FR	Framework Region
FRT	Flippase Recognition Target
GALT	Gut-associated lymphoid tissue
GC	Gene Conversion
HC	Heavy Chain
HRP	Horseradish Peroxidase
i.m.	Intramuscular
Ig	Immunoglobulin
IgH	Immunoglobulin heavy chain locus
JH	Junction segment Heavy Chain
JK	Junction segment Kappa Chain
PBMC	Peripheral Blood Mononuclear Cells
PBS	Phosphate-buffered Saline
PE	Phycoerythrin
RT	Room Temperature
SPR	Surface Plasmon Resonance
VH	Variable region Heavy chain
VK	Variable region Kappa chain

## Disclosure of Potential Conflicts of Interest

Francesca Ros, Sonja Offner, Stefan Klostermann, Irmgard Thorey, Helmut Niersbach, Sebastian Breuer, Grit Zarnt, Stefan Lorenz, Nicole Schueler, Tajana Dragicevic, Dominique Ostler, Imke Hansen-Wester, Valeria Lifke, Brigitte Kaluza, Klaus Kaluza, Alain C Tissot and Josef Platzer are or have been paid employees from Roche Diagnostics GmbH, and as such may hold equity in the company. Juergen Puels, Basile Siewe, Wim van Schooten and Roland Buelow indicate a conflict of interest statements obtained explicitly in writing from each author.

Affiliation: Roche Diagnostics GmbH for Roche and Therapeutic Human Polyclonals, Inc. for Wim van Schooten and Roland Buelow.

## Acknowledgments

We would like to thank Daniela Buntetuß, Marco Friedrich, Janine Gabler, Brigitte Huemer, Sabrina Kettenbach, Christoph Schuehlmann, Monika Lechner, Sven Krommelbein, Florie Greinhofer, Carolin Dirr, Nicole Reichenberger, Ireneus Jonetzko, Hildegard Moser, Friederike Jung, Frederic Schultz, Barbara Threm, Karlheinz Seitz, Olga Drews, Hedwig Ertl, Armin Schaub, Janine Koch und Janine Schlegel, Thomas Boehm and Christian Endter for their excellent technical assistance and helpful scientific discussion. We also thank the company Gene Bridges GmbH (Heidelberg), for the great collaboration on the Red/ET Recombination technology. Thanks to Jack Bates (Roche) for his reviewing help and finally we thank Rose Mage and Michael Neuberger for their precious scientific advisory on rabbit immunogenetics and overall project strategy and thanks to Christian Lehmann and Yvonne Kienast for their scientific support on Bmp9 biology.

## Author contributions

Overall study design and analysis of results were conducted by F.R., A.C.T., J.P., S.O., I.T., S.K.; H.N., S.B., G.Z., B.K., K.K., W.v.S. and R.B.; microinjection, embryo transfer, analysis of transgenic founders and lines, and immunizations were run by I.T. and I.H.W.; F.R., J.P., B.S., N.

S., T.D., D.O., I.H.W., J.P., contributed to the design, coordination, and conduction of the molecular biology activities. Breeding activities were planned and coordinated by H.N.; cloning and purification of recombinant BMP9 variants and pro-domain was supported by S.L.; serum analytics of transgenic rabbits was managed by S.O., I.T. and V.L.; S.O. was responsible for PBMC preparation, B cell sorting and cultivation; screening experiments were designed and conducted by K.K., S.B. and G.Z.; sequence analysis was supported by S.K. and F.R. The manuscript was written by F.R., S.O., S.K., I.T., H.N., S.B., G.Z., A.C.T.; all authors read and approved the submitted version.

## Funding

This study was funded by Roche Pharmaceutical Research and Early Development, Large Molecule Research, Roche Innovation Center Munich, Penzberg, Germany and initially by Therapeutic Human Polyclonals, Inc.

## References

- Kaplon H, Reichert J. Antibodies to watch in 2018. *mAbs*. 2018;10:183–203. doi:10.1080/19420862.2018.1415671.
- Chen W, Murawsky C. Strategies for generating diverse antibody repertoires using transgenic animals expressing human antibodies. *Front Immunol*. 2018;9:460. doi:10.3389/fimmu.2018.00460.
- Rossi S, Laurino L, Furlanetto A, Chinellato S, Orvieto E, Canal F, Facchetti F, Tos A. Rabbit monoclonal Antibodies A comparative study between a novel category of immunoreagents and the corresponding mouse monoclonal antibodies. *Am J Clin Pathol*. 2005;124:295–302. doi:10.1309/NR8HN08GDPVEMU08.
- Zhu W, Yu G-L. Rabbit Hybridoma. In: An Z, editors. *Therapeutic Monoclonal Antibodies: From Bench to Clinic*. John Wiley & Sons, Inc.; 2009. pp. 151–168.
- Knight KL. Restricted VH gene usage and generation of antibody diversity in rabbit. *Annu Rev Immunol*. 1992;10:593–616. doi:10.1146/annurev.iy.10.040192.003113.
- Lanning D, Zhu X, Zhai S, Knight K. Development of the antibody repertoire in rabbit: gut-associated lymphoid tissue, microbes, and selection. *Immunol Rev*. 2000;175:214–28. doi:10.1111/j.1600-065X.2000.imr017516.x.
- Mage R, Lanning D, Knight K. B cell and antibody repertoire development in rabbits: the requirement of gut-associated lymphoid tissues. *Dev Comp Immunol*. 2006;30:137–53. doi:10.1016/j.dci.2005.06.017.
- Kodangattil S, Huard C, Ross C, Li J, Gao H, Mascioni A, Hodawadekar S, Naik S, Min-debartolo J, Visintin A, et al. The functional repertoire of rabbit antibodies and antibody discovery via next-generation sequencing. *mAbs*. 2014;6:628–36. doi:10.4161/mabs.28059.
- Ros F, Puels J, Reichenberger N, van Schooten W, Buelow R, Platzer J. Sequence analysis of 0.5 Mb of the rabbit germline immunoglobulin heavy chain locus. *Gene*. 2004;330:49–59. doi:10.1016/j.gene.2003.12.037.
- Sehgal D, Johnson G, Wu T, Mage RG. Generation of the primary antibody repertoire in rabbits: expression of a diverse set of Igk-V genes may compensate for limited combinatorial diversity at the heavy chain locus. *Immunogenetics*. 1999;50:31–42. doi:10.1007/s002510050683.
- Brand V, Lehmann C, Umkehrer C, Bissinger S, Thier M, de Wouters M, Raemsch R, Jucknischke U, Haas A, Breuer S, et al. Impact of selective anti-BMP9 treatment on tumor cells and tumor angiogenesis. *Mol Oncol*. 2016;10:1603–20. doi:10.1016/j.molonc.2016.10.002.
- Kienast Y, Jucknischke U, Scheiblich S, Thier M, de Wouters M, Haas A, Lehmann C, Brand V, Bernicke D, Honold K, et al. Rapid activation of bone morphogenic protein 9 by receptor-mediated displacement of pro-domains. *J Biol Chem*. 2016;291:3395–410. doi:10.1074/jbc.M115.680009.

13. Mage R, Young-Cooper G, Alexander C, Kelus A. Genetics and expression of kappa-type light chains in Basilea rabbits. *Immunogenetics*. 1984;19:425–34. doi:10.1007/BF00364645.
14. Flisikowska T, Thorey I, Offner S, Ros F, Lifke V, Zeitler B, Rottmann O, Vincent A, Zhang L, Jenkins S, et al. Efficient Immunoglobulin gene disruption and targeted replacement in rabbit using zinc finger nucleases. *PLoS ONE*. 2011;6:e21045. doi:10.1371/journal.pone.0021045.
15. Seeber S, Ros F, Thorey I, Tiefenthaler G, Kaluza K, Lifke V, Fischer J, Klostermann S, Endl J, Kopetzki E, et al. A robust high throughput platform to generate functional recombinant monoclonal antibodies using rabbit B cells from peripheral blood. *PLoS ONE*. 2014;9:e86184. doi:10.1371/journal.pone.0086184.
16. Suzuki I, Pfister L, Glas A, Nottenburg C, Milner EC. Representation of rearranged VH gene segments in the human adult antibody repertoire. *J Immunol (Baltimore, Md: 1950)*. 1995;154:3902–11.
17. Parren PWIHW, Carter PJ, Plückthun A. Changes to international nonproprietary names for antibody therapeutics 2017 and beyond: of mice, men and more. *MAbs*. 2017;9:898–906. doi:10.1080/19420862.2017.1341029.
18. Abhinandan KR, Martin A. Analyzing the “Degree of Humanness” of antibody sequences. *J Mol Biol*. 2007;369:852–62. doi:10.1016/j.jmb.2007.02.100.
19. Ros F, Reichenberger N, Dragicevic T, Van Schooten WCA, Buelow R, Platzer J. Sequence analysis of 0.4 megabases of the rabbit germline immunoglobulin kappa1 light chain locus. *Anim Genet*. 2005;36:51–57. doi:10.1111/j.1365-2052.2004.01221.x.
20. Bergman Y, Rice D, Grosschedl R, Baltimore D. Two regulatory elements for immunoglobulin kappa light chain gene expression. *Proc Natl Acad Sci*. 1984;81:7041–45. doi:10.1073/pnas.81.22.7041.
21. Proudhon C, Hao B, Raviram R, Chameuil J, Skok J. Long-range regulation of V(D)J recombination. *Adv Immunol*. 2015;128:123–182.
22. Morvan C, Pinaud E, Decourt C, Cuvillier A, Cogné M. The immunoglobulin heavy-chain locus hs3b and hs4 3' enhancers are dispensable for VDJ assembly and somatic hypermutation. *Blood*. 2003;102:1421–27. doi:10.1182/blood-2002-12-3827.
23. Ferradini L, Gu H, De Smet A, Rajewsky K, Reynaud CA, Weill JC. Rearrangement-enhancing element upstream of the mouse immunoglobulin kappa chain J cluster. *Science (New York, NY)*. 1996;271:1416–20. doi:10.1126/science.271.5254.1416.
24. Lefranc G, Lefranc MP. Regulation of the immunoglobulin gene transcription. *Biochimie*. 1990;72:7–17.
25. Zou YR, Gu H, Rajewsky K. Generation of a mouse strain that produces immunoglobulin kappa chains with human constant regions. *Science (New York, NY)*. 1993;262:1271–74. doi:10.1126/science.8235658.
26. Brüggemann M, Davies NP, Rosewell IR. Designer mice: the production of human antibody repertoires in transgenic animals. *Year Immunol*. 1993;7:33–40.
27. Kurosawa K, Ohta K. Genetic diversification by somatic gene conversion. *Genes-basel*. 2011;2:48–58. doi:10.3390/genes2010048.
28. Reynaud C-A, Bertocci B, Dahan A, Weill J-C. Formation of the chicken B-cell repertoire: ontogenesis, regulation of ig gene rearrangement, and diversification by gene conversion. *Adv Immunol*. 1994;57:353–78.
29. Torres RM, Flawinkel H, Reth M, Rajewsky K. Aberrant B cell development and immune response in mice with a compromised BCR complex. *Science*. 1996;272:1804–08. doi:10.1126/science.272.5269.1804.
30. Cronin FE, Jiang M, Abbas AK, Grupp SA. Role of mu heavy chain in B cell development. I. Blocked B cell maturation but complete allelic exclusion in the absence of Ig alpha/beta. *J Immunol (Baltimore, Md: 1950)*. 1998;161:252–59.
31. Pruzina S, Williams G, Kaneva G, Davies S, Martín-López A, Brüggemann M, Vieira S, Jeffs S, Sattentau Q, Neuberger M. Human monoclonal antibodies to HIV-1 gp140 from mice bearing YAC-based human immunoglobulin transloci. *Protein Eng Des Sel*. 2011;24:791–99. doi:10.1093/protein/gzr038.
32. Reynaud S, Delpy L, Fleury L, Dougier H-L, Sirac C, Cogné M. Interallelic class switch recombination contributes significantly to class switching in mouse B cells. *J Immunol*. 2005;174:6176–83. doi:10.4049/jimmunol.174.10.6176.
33. Knight KL, Kingzette M, Crane MA, Zhai SK. Transchromosomally derived Ig heavy chains. *J Immunol (Baltimore, Md: 1950)*. 1995;155:684–91.
34. Kingzette M, Spieker-Polet H, Yam P-C, Zhai S-K, Knight K. Trans-chromosomal recombination within the Ig heavy chain switch region in B lymphocytes. *Proc Natl Acad Sci*. 1998;95:11840–45. doi:10.1073/pnas.95.20.11840.
35. Ma B, Osborn M, Avis S, Ouisse L-H, Ménoret S, Anegón I, Buelow R, Brüggemann M. Human antibody expression in transgenic rats: comparison of chimeric IgH loci with human VH, D and JH but bearing different rat C-gene regions. *J Immunol Methods*. 2013;400:78–86. doi:10.1016/j.jim.2013.10.007.
36. Osborn M, Ma B, Avis S, Binnie S, Dillej J, Yang X, Lindquist K, Ménoret S, Iscache A-L, Ouisse L-H, et al. High-affinity igg antibodies develop naturally in Ig-knockout rats carrying germline human IgH/Igk/Igλ loci bearing the rat CH region. *J Immunol*. 2013;190:1481–90. doi:10.4049/jimmunol.1203041.
37. Dougier H, Reynaud S, Pinaud E, Carrion C, Delpy L, Cogné M. Interallelic class switch recombination can reverse allelic exclusion and allow trans-complementation of an IgH locus switching defect. *Eur J Immunol*. 2006;36:2181–91. doi:10.1002/eji.200535529.
38. Dunnick W, Collins J, Shi J, Westfield G, Fontaine C, Hakimpour P, Papavasiliou N. Switch recombination and somatic hypermutation are controlled by the heavy chain 3' enhancer region. *J Exp Med*. 2009;206:2613–23. doi:10.1084/jem.20091280.
39. Shansab M, Eccleston J, Selsing E. Translocation of an antibody transgene requires AID and occurs by interchromosomal switching to all switch regions except the mu switch region. *Eur J Immunol*. 2011;41:1456–64. doi:10.1002/eji.201041077.
40. Newman BA, Young-Cooper CO, Alexander CB, Becker RS, Knight KL, Kelus AS, Meier D, Mage RG. Molecular analysis of recombination sites within the immunoglobulin heavy chain locus of the rabbit. *Immunogenetics*. 1991;34:101–09.
41. Schusser B, Yi H, Collarini E, Izquierdo S, Harriman W, Etches R, Leighton P. Harnessing gene conversion in chicken B cells to create a human antibody sequence repertoire. *PLoS ONE*. 2013;8:e80108. doi:10.1371/journal.pone.0080108.
42. Leighton P, Schusser B, Yi H, Glanville J, Harriman W, Diverse A. Repertoire of human immunoglobulin variable genes in a chicken B cell line is generated by both gene conversion and somatic hypermutation. *Front Immunol*. 2015;6:126.
43. Ching K, Collarini E, Abdiche Y, Bedinger D, Pedersen D, Izquierdo S, Harriman R, Zhu L, Etches R, van de Lavoie M-C, et al. Chickens with humanized immunoglobulin genes generate antibodies with high affinity and broad epitope coverage to conserved targets. *Mabs*. 2017;10:71–80.
44. Mage R, Sehgal D, Schiaffella E, Anderson A. Gene-conversion in rabbit B-cell ontogeny and during immune responses in splenic germinal centers. *Vet Immunol Immunopathol*. 1999;72:7–15. doi:10.1016/S0165-2427(99)00110-5.
45. Schiaffella E, Sehgal D, Anderson AO, Mage RG. Gene conversion and hypermutation during diversification of VH sequences in developing splenic germinal centers of immunized rabbits. *J Immunol (Baltimore, Md: 1950)*. 1999;162:3984–95.
46. Mehr R, Edelman H, Sehgal D, Mage R. Analysis of mutational lineage trees from sites of primary and secondary ig gene diversification in rabbits and chickens. *J Immunol*. 2004;172:4790–96. doi:10.4049/jimmunol.172.8.4790.
47. Rousseeuw P, Hubert M. Robust statistics for outlier detection. *Wiley Interdiscip Rev*. 2011;1:73–79.
48. Li M, Elledge S. Harnessing homologous recombination in vitro to generate recombinant DNA via SLIC. *Nat Methods*. 2007;4:251–56. doi:10.1038/nmeth1010.
49. Haun RS, Serventi IM, Moss J. Rapid, reliable ligation-independent cloning of PCR products using modified plasmid vectors. *BioTechniques*. 1992;13:515–18.
50. Rousseeuw P. Silhouettes: A graphical aid to the interpretation and validation of cluster analysis. *J Comput Appl Math*. 1987;20:53–65. doi:10.1016/0377-0427(87)90125-7.